Active stabilization studies at the sub-nanometer level for future linear colliders

N. Geffroy, L. Brunetti, B. Bolzon, A. Jérémie, B. Caron, J. Lottin

LAPP-TECH-2008-03
September 2008

Active stabilization studies at the sub-nanometer level for future linear colliders

N. Geffroy, L. Brunetti, B. Bolzon, A. Jérémie

LAPP - Université de Savoie - IN2P3-CNRS
BP. 110, F-74941 Annecy-le-Vieux Cedex, France

B. Caron, J. Lottin

Laboratoire SYstèmes et Matériaux pour la MEcatronique
BP. 80439, F-74944 Annecy-le-Vieux Cedex, France

Presented by **N. Geffroy**
at Mecatronics 2008, 7th France-Japan (5th Europe-Asia) Congress on Mechatronics, Le Grand Bornand (France), 21-23 May 2008

Active stabilisation studies at the sub-nanometre level for future linear colliders

N.Geffroy[1], L.Brunetti[1], B.Bolzon[1], A.Jeremie[1], B.Caron[2], J.Lottin[2]
[1]LAPP-IN2P3-CNRS-Université de Savoie and [2]SYMME-Polytech'Savoie-Université de Savoie
chemin de Bellevue, Annecy-le-Vieux, France
Nicolas.Geffroy@lapp.in2p3.fr

***Abstract*-The next collider which will be able to contribute significantly to the comprehension of matter is a high energy linear collider. The luminosity of this collider will have to be of $10^{35}cm^{-2}s^{-1}$, which imposes a vertical beam size of 0,7nm. The relative motion between the last two focusing magnets should not exceed a third of the beam size above 4Hz. Ground motion and acoustic noise can induce vibrations that have to be compensated with active stabilisation. In this paper, we describe the three aspects needed for such a development. We have assessed sensors capable of measuring sub-nanometre displacements, performed numerical calculations using finite element models to get the dynamic response of the structure, and developed a feedback loop for the active stabilisation. Combining the expertise into a mecatronics project made it possible to obtain a displacement RMS at 5Hz of 0.13nm at the free end of our prototype.**

I. Introduction

Probing the infinitely small requires large instruments like particle accelerators. The next collider which will be able to contribute significantly to the comprehension of matter is a high energy linear collider, with energy of the order of 1TeV. Two projects of are being studied today, CLIC and ILC. The CLIC collider will be composed of two arms of approximately 16km which face each other and in which an electron beam and a positron beam will be accelerated before colliding with each other in the centre of this machine. The luminosity of this collider will have to be of $10^{35}cm^{-2}s^{-1}$, which imposes a vertical beam size of 0,7nm. In order to maximise the luminosity at the interaction point, the relative motion between the last two focusing magnets, the final doublets, should not exceed a third of the beam size above 4Hz [1].

Major vibration sources like ground motion [2] and acoustic noise can induce displacements of a few nanometres above 4Hz. Thus, an active stabilization of the ground and of the final doublets at their resonance frequencies must be carried out [3].

First, in order to stabilize final doublets to the sub-nanometre level, we have to compensate for the nanodisplacements induced by cultural noise. We consequently need sensors and actuators which are able to measure and create displacements of mechanical structures at the sub-nanometre level while being placed in a harsh environment composed of high magnetic fields and radiation. We also need a feedback loop which controls actuators from sensor data. In addition, mechanical simulations and dynamic response calculations are included in this study for defining the active stabilisation feedback loop.

II. Sensor assessment

We started by assessing very sensitive, commercial vibration sensors, acquisition systems and signal conditioning for displacement measurements at the sub-nanometre level.

A. Instrumentation

When measuring nanodisplacements, resolution of the measurement chain is limited by internal noise of the chain itself, mainly composed of sensors and acquisition system noises. Consequently, these noises have been measured to evaluate sensors' and acquisition systems' performances. In table I and table II, the characteristics and the measured noise of the three types of vibration sensors used by our team are given.

B. Low frequency vibrations

Two types of commercial vibration sensors which are liable to measure nanodisplacements have been acquired: electromagnetic geophones using a servo loop to control the mass position and piezoelectric accelerometers coupled with sensitive charge amplifiers.

TABLE I
GEOPHONE CHARACTERISTICS

Type of geophones	**Electromagnetic**	**Electrochemical**
Model	GURALP CMG-40T	SP500-B
Company	Geosig	PMD Scientific
Sensitivity	1600V/m/s	2000V/m/s
Range (Hz)	[0.033; 50]	[0.0167; 75]
Measured noise for f>4Hz (nm)	0.05	0.06

TABLE II
ACCELEROMETER CHARATERISTICS

Type of sensors	**Piezoelectric accelerometers**	
Model	ENDEVCO 86	393B12
Company	Brüel & Kjaer	PCB Piezotronics
Sensitivity	10V/g	10V/g
Range (Hz)	[0.01;100]	[0.15; 1000]
Measured noise for f>4Hz (nm)	0.38 >50Hz: 0.02	17.5 >300Hz: 0.005

Because one measures velocity and the other measures acceleration, performances of these two types of sensors were compared to know in which frequency range they are the most sensitive with respect to ground motion.

Two GURALP geophones [4] and two ENDEVCO accelerometers [5] have been put side-by-side on the floor and their signals registered by an acquisition system (PULSE system [6] from Brüel & Kjaer Company) of very low noise due to its integrated state-of-the-art electronics,.

From these measurements, coherences [7] between the signals of the two GURALP sensors and of the two ENDEVCO sensors have been calculated. A bad coherence means that signals are contaminated by instrumental noise because ground motion is coherent between two points close to each other and instrumental noise is not. Also, signal to noise ratios of these two types of sensors have been calculated for consistency. Results are shown in fig.1.

Signal to noise ratios and coherences of GURALP sensors are very good from 0.1Hz up to the upper limit of their frequency range (50Hz) but the ones of ENDEVCO sensors are good only above 5Hz.

Note that there is a very good consistency of results between signal to noise ratios and coherences even if calculations of coherences and of noises are from different measurements. The first calculation is from coherence measurements done the day. The noise measurements are done the night in order to get less ground motion signals and to have consequently a better estimation of sensor noise. This shows that the noise estimation done by either method gives good results.

To understand such difference of performances at low frequency between these two types of sensors, raw signals have to be analyzed because accelerometers measure acceleration and geophones measure velocity. In fig.2, the solid and solid thick curves represent respectively Power Spectral Density (PSD) [7] of ground velocity measured by GURALP geophones and PSD of ground acceleration measured by ENDEVCO accelerometers. The dashed and dash-dot curves represent respectively PSD of measured noises. As shown above, because PSD of ground acceleration could not be measured by ENDEVCO sensors at low frequencies, PSD of ground acceleration (dotted curve) has been computed by deriving ground velocity measured by GURALP sensors.

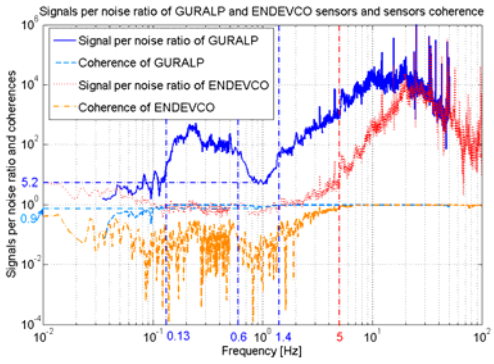

Fig 1: Signal to noise ratio of GURALP and ENDEVCO and coherences

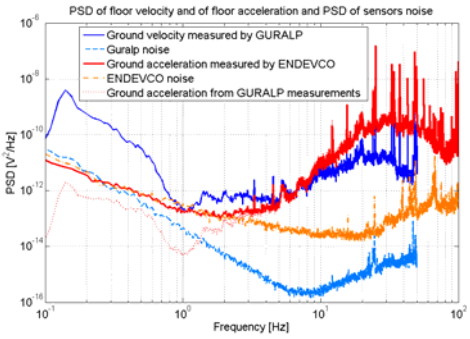

Fig.2. PSD of floor velocity, of floor acceleration and of sensors noise

At low frequencies, ground acceleration is very low compared to ground velocity and is below sensor noises (identical for both types of sensors), which explains why signal to noise ratio and coherence of ENDEVCO sensors were very bad. That means that ground motion has to be measured by geophones below 1Hz and can be measured by both types above a few Hertz. In order to perform different vibratory studies in a wide frequency range, for instance ground motion study or evaluation of the STACIS commercial active isolation system presented in fig.6, we use GURALP geophones to measure vibrations below 1Hz to 50Hz and ENDEVCO accelerometers to measure vibrations from a few Hertz up to 100Hz.

C. High frequency vibrations

Another model of accelerometers, the high frequency 393B12 accelerometers [8], has been acquired by our team to perform vibratory studies of a cantilever beam at high frequencies (above 300Hz). The goal is to know up to which frequency a stabilization has to be done since ground motion decreases with frequency and since acoustic noise can be important at high frequencies.

Fig.3 represents the floor acceleration PSD measured by these sensors with the PSD of their measured noise (left plot) and the signal to noise ratio of the sensors with their coherence (right plot).

Ground acceleration increases above 200-300Hz and 393B12 noise decreases with frequency, which allows having a high signal to noise ratio and consequently accurately measuring ground motion at high frequencies. This is confirmed by the good coherence obtained above the same frequency. Note that signal to noise ratio and coherence results are consistent as mentioned in the *Instrumentation* section.

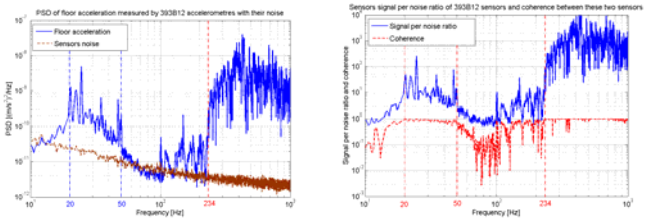

Fig.3. Floor acceleration PSD measured by 393B12 sensors with their noise PSD (left) and signal to noise ratio of the sensors with their coherence (right)

D. *Sensors for active rejection*

Because electromagnetic geophones and piezoelectric accelerometers are sensitive to high magnetic fields and to radiations, a collaboration with PMD Scientific Company and SLAC laboratory has been created to develop electrochemical vibration sensors, the SP500 sensors [9], not sensitive to such environment for the active stabilisation of the future linear collider final doublets.

To know if their sensitivity is sufficient, SP500 noise has been measured with the PULSE system. For that, we acquired data for the complete measurement chain by using the Corrected Difference method [10]. For the PULSE system noise, measurements were done by putting 50 ohm adapters on its inputs. By subtracted PULSE noise to the measurement chain noise, we obtained SP500 noise. Results of integrated Root Mean Square (RMS) [11] of the measurement chain noise and of the SP500 noise are given in fig.4.

This figure shows that noises of the measurement chain and of SP500 sensors are quite the same and are of 0.06nm above 4Hz. This means that PULSE system has a very low noise compared to sensor noise and consequently doesn't degrade sensor performances, and that these sensors are able to measure sub-nanometre displacements.

A basic acquisition system (the DAQ PCI6052E from NI [12]) but compatible with Matlab/Simulink (the software used to develop our feedback loop) allows us to measure displacements with SP500 sensors from 0.14nm to 500nm above 4Hz thanks to some adapted home-made filters and some amplifiers integrated in the acquisition system. This dynamic range is sufficient to measure vibrations of structures subjected to ground motion down to the sub-nanometre level and this measurement chain has been consequently used in the vibration active rejection of our prototype.

Now that the sensor performances have been found to be compatible with sub-nanometre measurements, numerical calculations of the whole system have been performed.

III. Numerical simulations

Numerical simulations can be a great help to test the efficiency and the robustness of the active control algorithm in realistic conditions. The main objective is to obtain a state-space model of the structure to control, in order to use it in Matlab/Simulink to get dynamic response of this structure under predefined loads.

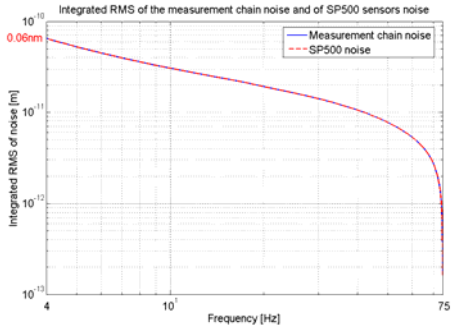

Fig.4. Integrated RMS of the measurement chain noise and of SP500 noise.

To do this the first step can be the finite element modelling of the structure.

A. *Finite Element Model*

Finite element modelling is of prime importance, insofar as the finite element model is required for the future results to be representative. Indeed, the state-space model will use the formulations of the finite element model (FE model). In order to get the most realistic results (in terms of dynamic and control), the FE model must be as accurate as possible.

Consequently, updating the FE model is a step of the utmost importance. Thus, experimental vibration measurements are required to get, on the one hand the different eigenfrequencies and their corresponding mode shapes, and on the other hand their level of damping. Then a model updating can be performed.

Note that most of the time, the use of Super-Element can be realized to reduce the size of the system to solve, which is a non-negligible aspect for the future dynamic computations.

B. *State-Space Model*

The State-Space model results exclusively from the FE model (1), namely the mass, damping and stiffness matrices without forgetting the external applied loads. The latter act as the input of the model, the output being the motion of some predefined locations (in terms of acceleration, velocity and displacement). The fundamental equation describing the dynamic behavior of a structure is:

$$M\ddot{q}(t) + B\dot{q}(t) + Kq(t) = g(t) \qquad (1)$$

where the q(t) state vector collects the displacements of the structure by degree of freedom, while the g(t) vector indicates the corresponding applied loads.

The state-space model will have the following form, assuming that only external forces can be applied to the model:

$$\begin{cases} \dot{x} = Ax + Bu \\ y = Cx + Du \end{cases} \qquad (2)$$

where the state vector x, the input vector u and the output vector y are defined as:

$$x = \begin{Bmatrix} q \\ \dot{q} \end{Bmatrix} \qquad u = \{F\} \qquad y = \begin{Bmatrix} q_{out} \\ \dot{q}_{out} \\ \ddot{q}_{out} \\ F_{out} \end{Bmatrix} \qquad (3)$$

According to (1), the acceleration vector can be written as follows

$$\ddot{q} = -M^{-1}B\dot{q} - M^{-1}Kq + M^{-1}F \qquad (4)$$

Finally, the different matrices are defined below, assuming that only external forces can be applied to the model:

$$A=\begin{bmatrix} 0 & I \\ -M^{-1}K & -M^{-1}B \end{bmatrix} \qquad B=\begin{bmatrix} 0 \\ M^{-1} \end{bmatrix}$$
$$C=\begin{bmatrix} I & 0 \\ 0 & I \\ -M^{-1}K & -M^{-1}B \\ 0 & 0 \end{bmatrix} \qquad D=\begin{bmatrix} 0 \\ 0 \\ M^{-1} \\ I \end{bmatrix} \qquad (5)$$

In the general method, it is assumed that only external forces are applied to the structure. Nevertheless, an extended method has been proposed [13], in which external disturbances can be not only pinpoint forces, but also prescribed acceleration for instance.

In a FE code, the dynamic response of a structure under prescribed acceleration $\ddot{q}_2(t)$ is computed according to the following way. First, the corresponding prescribed velocities and displacements are numerically integrated:

$$\dot{q}_2(t)=\int_0^t \ddot{q}_2(\tau)\cdot d\tau \text{ and } q_2(t)=\int_0^t \dot{q}_2(\tau)\cdot d\tau \qquad (6)$$

Then the system to solve is now written:

$$\begin{bmatrix} M_{11} & M_{12} \\ M_{21} & M_{22} \end{bmatrix}\begin{Bmatrix} \ddot{q}_1 \\ \ddot{q}_2 \end{Bmatrix}+\begin{bmatrix} B_{11} & B_{12} \\ B_{21} & B_{22} \end{bmatrix}\begin{Bmatrix} \dot{q}_1 \\ \dot{q}_2 \end{Bmatrix}+\dots$$
$$\dots\begin{bmatrix} K_{11} & K_{12} \\ K_{21} & K_{22} \end{bmatrix}\begin{Bmatrix} q_1 \\ q_2 \end{Bmatrix}=\begin{Bmatrix} g_1(t) \\ -r_2(t) \end{Bmatrix} \qquad (7)$$

where the index 2 stands for the *dof* where acceleration is applied and index 1 for all other *dof* of the model. Moreover, $g_1(t)$ represents the possible external point forces. The first equation of the system (7) allows the dynamic response computation, provided one carries over the right hand side forces of inertia, dissipation and stiffness associated with the prescribed motion:

$$M_{11}\cdot\ddot{q}_1+B_{11}\cdot\dot{q}_1+K_{11}\cdot q_1=\dots$$
$$\dots g_1(t)-M_{12}\cdot\ddot{q}_2-B_{12}\cdot\dot{q}_2-K_{12}q_2 \qquad (8)$$

Hence, in a general way, the input vector u of the state-space model will put together the terms of point forces and the terms of forces of inertia, dissipation and stiffness, which corresponds to the right hand side terms of (8).

Finally, by correctly initializing the different matrices of the State-Space model in Simulink, it is possible to get the dynamic response of the structure under prescribed acceleration. The active control can be coupled to this computation by adding for instance pinpoint forces (if pinpoint actuators are required) in the input vector of the state-space model.

The active control algorithm will be described in the next section.

IV. Active stabilization

In order to obtain a very low displacement of the two final doublets of the future linear collider, of about 1/3 of the beam size in the vertical axis in a desired range of 4 – 100Hz, a lot of constraints have to be considered. The complexity of the mechanical structure and the multitude of perturbation sources are the two main aspects of this problem.

Concerning the mechanical structure, the design of the future linear collider is not yet finalised. However, this will be very complex, so a few intermediate stages are necessary. This is why this study aims to obtain a very low displacement all along an elementary mechanical structure which is similar to the future final doublet in the main aspects that concern our work. The prototype used for this experiment is a 2,5m long steel beam in cantilever mode, respecting the elementary parameters planned for the final doublet. Furthermore, the eigenfrequencies of this linear structure are included in the desired range. The measurement of the motion is performed with the velocity sensor SP500 presented in the *sensor assessment* part. Concerning the actuators, assemblies of piezoelectric patches (APA 25XS from the CEDRAT Company) are used. They allow creating very low displacements at a nanometre scale all along the beam. The built prototype is presented in fig.5.

In order to attenuate the motion of this prototype, the influence of the perturbations has to be analysed. In fact, there are two types of motions that can be identified:

- The vertical motion of the clamping created by the ground motion. Their effects excite indirectly the mechanical structure, mainly its resonant modes.
- The motion of the mechanical structure itself created by acoustic perturbations which excite it in all directions.

In order to deal with the two aspects of the problem, two methods are used. First of all, the purpose of our study is to obtain a very low displacement of the clamping by the use of passive and active isolation, in order to isolate the whole system from the ground motion [14]. For that, an industrial active table has been tested [15]. This is an active table produced by the company TMC with 4 STACIS active isolators (fig.6). Even if this table is really efficient (For example: 3 nanometers with table OFF vs. 0.2 nanometers table ON), this solution is not sufficient given the very strict allowed tolerances (1/3 nm).

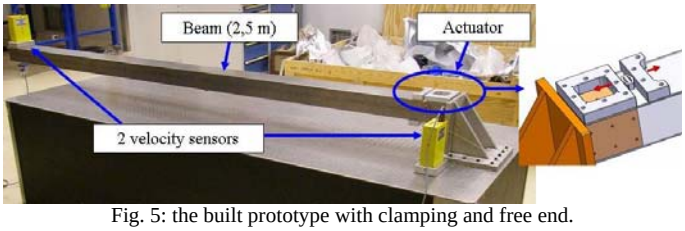

Fig. 5: the built prototype with clamping and free end.

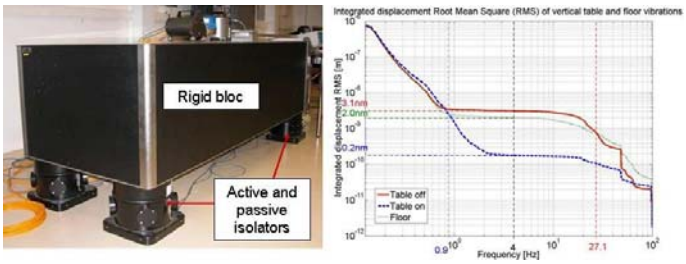

Fig. 6: The active table TMC and an example of an obtained integrated displacement RMS

Indeed, this approach does not consider the acoustic perturbations and even the slightest motion of the clamping will be amplified by the structure, mainly for its resonant modes. This is why active compensation has been developed and the approach and the results are presented in this paper. The proposed method consists in applying a force that creates a motion in opposition with the motion created by the perturbations. This will maintain the mechanical structure in a straight horizontal position along its axis.

Two algorithms have been developed. Because of the complexity of the structure, it is considered that it is too complicated to compute a fine model representative of the system. The originality of the proposed algorithms is that each of them takes into consideration only the measurable behaviour of the system and that they do not require an accurate complete model of the structure.

The first algorithm is based on a state space representation as described in fig.7 and is dedicated to lumped perturbation [16].

After the simulation stage described in the previous section, this algorithm was evaluated on the large prototype at a nanometer scale. Fig.8 represents the result of the stabilization, more precisely the amplitude spectral density of the displacement at the end of the beam in a natural environment, without adding any external disturbances. The first two modes of flexion of the beam can be recognized (large peaks) and a lot of unknown other disturbances can be noticed (narrow peaks). For the presented illustration, one of the narrow peaks has been arbitrarily selected (the surrounded peak) and we can see that the rejection is efficient. It is possible to parallelize the algorithms that reject each of these narrow peaks, in order to reduce as much as possible the motion of the mechanical structure.

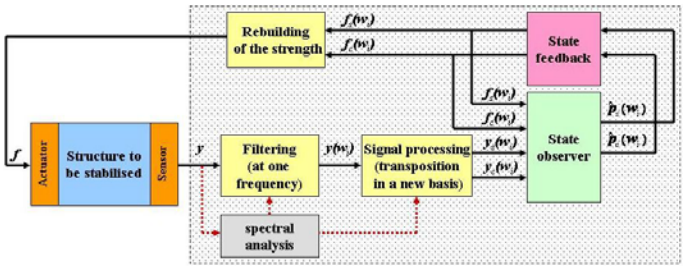

Fig. 7: The first developed algorithm for active compensation

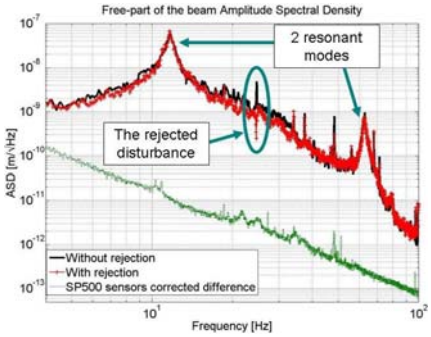

Fig. 8: ASD of the displacement at the end of the beam with and without rejection

As a conclusion, we can state that this algorithm is able to reject narrow peaks at a nanometre scale. However, for the eigenfrequencies, this method is quite limited, because working at a given frequency does not allow treating a bandwidth.

Considering these remarks, a second algorithm was developed. It is based on a command with internal model [17]. In order to meet the needs of our specific problem of stabilization, this method was adapted. In fact, the proposed algorithm uses only an elementary model which is representative for the structure behaviour and for a given bandwidth corresponding to a resonant mode. For the purpose of controlling all the desired range, there are as many algorithms as there are frequencies or bandwidths to process. The adaptation of the command with internal model control for one bandwidth is described in the fig.9.

As previously, this algorithm was tested in simulation, then with the large prototype in a natural environment. Two bandwidths were processed, each of them corresponding to a resonant mode of the mechanical structure (12 and 68 Hz). Fig.10 represents the transfer function between the measured displacement at the end of the beam and the measured displacement at the clamping, with and without rejection (left plot) and the integrated displacement root mean square at the clamping and at the end of the beam with and without rejection (right plot).

These results reveal that for the two treated bandwidths the algorithm is efficient, since the amplification is considerably reduced. However, the results can be improved, because the processing of a bandwidth has a small detrimental influence on neighbouring frequencies. Considering these results, the combination of active compensation with active isolation was tested in order to investigate if the approach can be applied at a sub-nanometre scale.

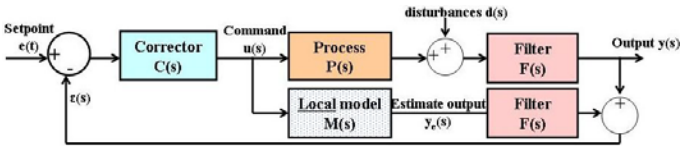

Fig. 9: Adaptation of a classic command with internal model control

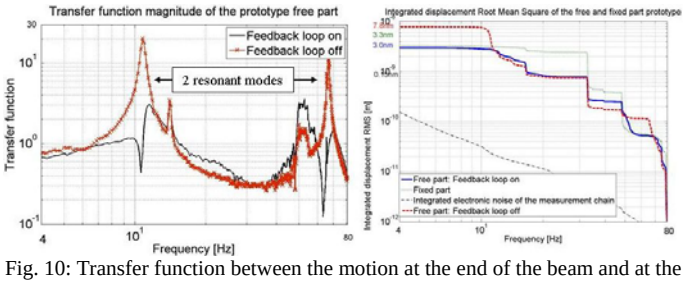

Fig. 10: Transfer function between the motion at the end of the beam and at the clamping (left) and the integrated displacement RMS with and without rejection (right)

In this prospect, the prototype was fixed on the active table. Fig.11 represents the obtained results.

Because of the active isolation, the measured displacement at the end of the beam (without active compensation) is lower than a nanometre (0.25 nm). Even if this displacement is already very low, we also apply the active compensation and the obtained results reduce the motion at approximately the same ratio as before. The result is a very low displacement, actually an absolute stabilization about a tenth of nanometre. This test proves that the instrumentation is not a limitation and that it is possible to stabilize at the tenth of nanometre scale. The next objective is to obtain these results not only on a selected point of the beam, but all along its length.

V. Conclusion

Thanks to some electrochemical vibration sensors and piezoelectric actuators associated with an appropriate instrumentation, a control algorithm developed by our team and a real time apparatus, the feasibility of actively rejecting structure vibrations down to 0.1Hz has been proven by using in parallel a commercial system performing passive and active stabilization of the clamping. The design of the linear collider final doublets is not finished but the tools developed by our team, including the simulation of the whole system, will allow us to follow their evolution. Moreover, the mechanical modelling will give us information about optimal location of sensors and actuators for the active rejection of structures all along their length.

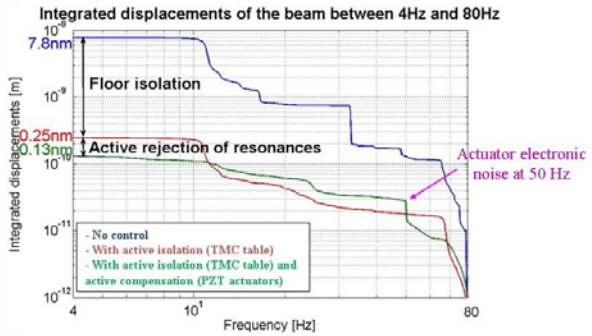

Fig. 11: Integrated displacement RMS obtained with the combination of active compensation and active isolation

Acknowledgment

This work is supported by the Commission of the European Communities under the 6th Framework Programme "Structuring the European Research Area", contract number RIDS-011899.

References

[1] S. Redaelli, "Stabilization of Nanometre-size Particle Beams in the Final Focus System of the Compact Linear Collider (CLIC)," PhD Thesis, Université de Lausanne, 2003, 194 pages, also as CERN-AB-2004-025

[2] A. Seryi, O. Napoly, "Influence of ground motion on the time evolution of beam in linear colliders", DAPNIA/SEA 95 04, Août 1995

[3] C. Montag, "Active stabilization of mechanical quadrupole vibrations for linear colliders", Nuclear Instruments and Methods in Physics Research, A 378 (1996) 369-375

[4] http://www.geosig.com/downloads/leaflets/L_CMG-40T.pdf

[5] http://www.bksv.com/pdf/86.pdf

[6] http://www.bksv.com/pdf/Bu0228.pdf

[7] National Instruments, "The Fundamentals of FFT-Based Signal Analysis and Measurement in LabVIEW and LabWindows/CVI", Document Version 4, 2006

[8] http://www.pcb.com/contentstore/docs/PCB_Corporate/Vibration/Products/Manuals/393B12.pdf

[9] http://www.pmdsci.com/pdfs/LC501.pdf
http://www.eentec.com/SP-500_data.htm

[10] Zeroth Order Design Report for the NLC, "Ground Motion: Theory and Measurement", Appendix C: Ground motion, theory and measurements

[11] Dr. Peter G. Nelson, "Understanding and Measuring Noise Sources in Vibration Isolation Systems", VP/CTO Technical Manufacturing Corporation, July 2003

[12] http://www.ni.com/pdf/products/us/4daqsc199-201_ETCx3_212-213.pdf

[13] N. Geffroy, L. Brunetti, B. Bolzon, A. Jeremie , J.Lottin, "Creation of a State-Space Model from a Finite Element Model for the active control algorithm efficiency tests", EUROTeV-Report-2007-054

[14] M. R. Bai and W. Liu, "Control Design of Active Vibration Isolating using μ-Synthesis", Journal of Sound and Vibration, 257(1), (2002) 157-175.

[15] TMC Company, "TMC STATIS 2000 STABLE ACTIVE CONTROL ISOLATION SYSTEM", Users manual, Document P/N 96-26690-02 Rev. D, Novembre 2002

[16] C.Adloff, B.Bolzon, F.Cadoux, N.Geffroy, S.Géneté, C.Girard, A.Jeremie, Y.Karyotakis, L.Brunetti, J.Lottin Vibration stabilization for the final focus magnet of a future linear collider, proc. REM 2005 conference, Annecy-le-Vieux, June30-July1, 2005 or LAPP-TECH-2005-01

[17] Y. -S. Lee and S. J. Elliott, "Active position control of a flexible smart beam using internal model control", Journal of Sound and Vibration 242, Issue 5, 2001, pp 767-791.